BFKL resummation effects at Hadron Colliders

Federico M. Deganutti, Christophe Royon, Dimitri Colferai

The University of Kansas,The University of Florence

The Energy Frontier, Snowmass Meeting

fedeganutti@ku.edu

September 30, 2020

- Balitsky, Fadin, Kuraev, Lipatov (BFKL) resummation
- BFKL vs DGLAP
- Mueller-Navelet jets at LHC
- Mueller-Tang jets at Tevatron and LHC
- Jet gap jet: full NLL calculation (kernel and impact factor)

BFKL as low-x resummation kernel

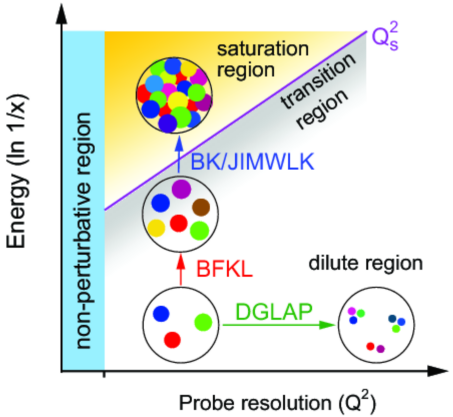

BFKL evolution kernel toward small-x ($x = x_{\mathcal{B}}$). **Forward emission**. DGLAP evolution kernel towards increasing probe resolution Q^2 at fixed energy $x_{\mathcal{B}}$. Both necessary to explain the QCD parton densities (including the small-x region).

BFKL is part of global PDF fits

First hint of low-x resummation effects (BFKL dynamics) extracted from Hera data[1710.05935v2 [hep-ph]].

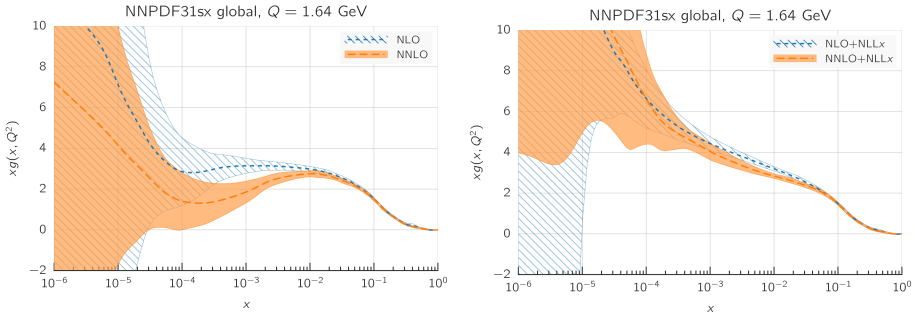

Gluon NNPDF3.1 PDF. Global fit to Hera data.

The PDFs obtained with small-x resummation using NLO+NLLx and NNLO+NLLx theory are in much closer agreement with each other at medium and small x than the corresponding fixed-order NLO and NNLO PDFs. The theoretical uncertainty due to missing higher order corrections in a NNLO+NLLx resummed calculation is rather less at small x than that of the fixed-order NNLO calculation. fixed-order calculations have a perturbative instability at small x due to large logarithms that can be cured by resummation.

PDFs uncertainties often dominates the error bands for hadron collisions.

High energy limit of QCD

BFKL effects are predicted to dominate in *Semi*-hard regimes: $s \gg -t \gg \Lambda_{QCD}$
Despite Q : $\alpha_S(Q^2) \ll 1$ whole string of sub-leading diagrams must be resummed if $\alpha_S(Q^2)\log\left(\frac{s}{Q^2}\right) \simeq 1$.

Radiative corrections of order n to the partonic cross sections

$$d\hat{\sigma} \simeq \alpha_s^n \log^n\left(\frac{s}{-t}\right) A + \alpha_s^n \log^{n-1}\left(\frac{s}{-t}\right) B + \ldots$$

The perturbative expansion breaks down when $\alpha_s^2 \log^2 s/t \simeq \alpha_s \log s/t$

- *New hierarchy divides the diagrams of the perturbative expansion*
- Leading logarithmic approximation (LL):
  $\alpha_s^n \log^n\left(\frac{s}{-t}\right)$, $n = 1, 2, \ldots$
- Next-to-leading logarithmic approximation (NLL):
  $\alpha_s^n \log^{n-1}\left(\frac{s}{-t}\right)$, $n = 1, 2, \ldots$

Pomeranchuk Th: *The color singlet exchange dominates at high energies.*

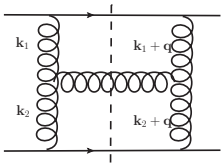

Figure: Diagram enhanced by **one** power of the large logarithms.

BFKL vs DGLAP

Resumming distinct subset of Feynman diagrams to all orders of perturbation theory. (Almost) Complementary limit of QCD. Overlapping not easy to disentangle.

- DGLAP: resum terms $\propto \log \frac{Q}{\lambda} \gg 1$. Q = exchanged momentum, λ = factorization scale.
- BFKL: resum terms $\propto \log \frac{s}{-t} \gg 1$. s = center-of-mass energy, $-t = Q^2$.

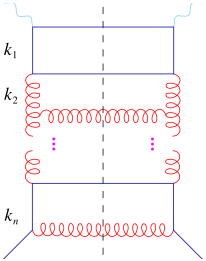

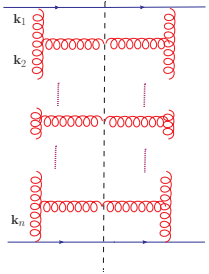

- Phase space DGLAP LO

$$\boxed{\mathbf{k}_1 \gg \mathbf{k}_2 \gg \cdots \gg \mathbf{k}_n} \qquad y_1 \simeq y_2 \simeq \cdots \simeq y_n$$

- Phase space BFKL LL

$$\boxed{y_1 \gg y_2 \gg \cdots \gg y_n} \qquad \mathbf{k}_1 \simeq \mathbf{k}_2 \simeq \cdots \simeq \mathbf{k}_n$$

BFKL equation

Recursive integral equation in the form of a Green function equation called BFKL equation. The ladder diagrams are resummed to all order in the Gluon Green function G.

$$G(\mathbf{k},\mathbf{k}') = \delta^2(\mathbf{k}-\mathbf{k}') + \int d^2\ell \mathcal{K}(\mathbf{k},\ell) G(\ell,\mathbf{k}')$$

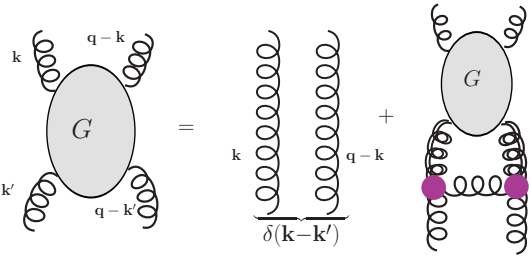

$$G(\mathbf{k},\mathbf{k}',\mathbf{q},Y) = \int_{-i\infty}^{+i\infty} \frac{d\omega}{2\pi i} e^{Y\omega} \sum_{n\in\mathcal{Z}} \int_{\frac{1}{2}-i\infty}^{\frac{1}{2}+i\infty} \frac{d\gamma}{2\pi\, i} \frac{E_{\gamma,n}(k) E^*_{\gamma,n}(k')}{\omega - \bar{\alpha}_s \chi(\gamma,n)} \qquad e^{Y\omega} = \left(\frac{s x_1 x_2}{-t}\right)^{\omega}$$

$$E_{n,\nu} \propto \begin{cases} {}_2F_1\Big(a(n,\nu), b(n,\nu), c, z(\mathbf{k},\mathbf{k}')\Big), & \text{Gauss hypergeometric function} \\ |\mathbf{k}|^{-\frac{1}{2}+i\nu} e^{in\theta}, & \text{forward limit } \; q \to 0. \end{cases}$$

Mueller-Navelet Jets

Mueller Navelet jets as preferred testing ground for BFKL dynamics.
$p + p \to jet_1 + jet_2 +$ anything else
Tagged jets far apart in rapidity.
High energy factorization separates the probe dependent jet vertices from the universal Gluon Green function.

$$\frac{d\sigma}{dJ_1 dJ_2} = V_a(\mathbf{k}_{J_1}, x_{J_1}, \mathbf{k}_1) \otimes G(\mathbf{k}_1, \mathbf{k}_2, \hat{s}) \otimes V_b(\mathbf{k}_{J_2}, x_{J_2}, \mathbf{k}_2)$$

Convolution in $(\mathbf{k}, x)$.
Observables: cross section and azimuthal (de)correlation.

- $C_0 = \frac{d\sigma}{dY}$
- $\frac{C_m}{C_0} = \langle \cos(m\Delta\phi_J) \rangle$

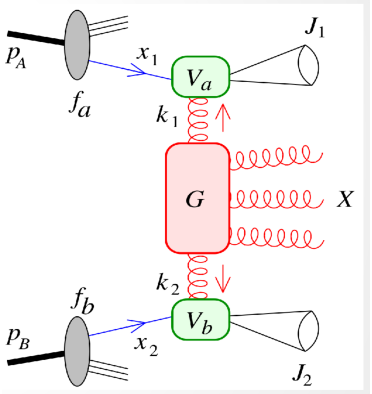

$$C_m(Y) = \int dy_1 dy_2 \delta(y_1 + y_2 - Y) d^2\mathbf{k}_{J_1} d^2\mathbf{k}_{J_2} \cos(m(\phi_{J_1} - \phi_{J_2} - \pi)) \frac{d\sigma}{dJ_1 dJ_2}$$

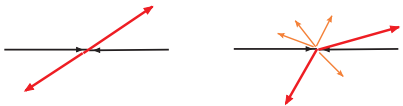

BFKL induced decorrelation dominates over DGLAP [C. Marquet, C.Royon, Phys. Rev. D79 (2009) 034028]

CMS Analysis

Test of BFKL predictions at $\sqrt{s} = 7$ TeV for the first moments of the average cosines C_n/C_0 compared to the DGLAP predictions [J. High Energy Phys. 08 (2016) 139]

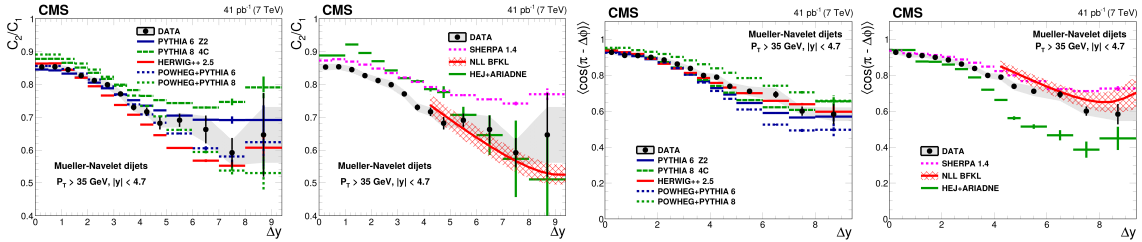

- Full NLL BFKL including NLO vertices and collinear resummation leads to a good description of $\langle \cos(n\Delta\phi) \rangle$ data but also PYTHIA/HERWIG after MPI tuning.
- Study of C_2/C_1 fails to provide any sensible advantage.
- More differential observables needed or completely new ones

Less inclusive Observables

Mini-jets activity should allow a better discrimination of BFKL and DGLAP dynamics.
Need BFKLex iterative MC generator [A. Sabio-Vera, G. Chachamis, JHEP02 064 (2016)].

BFKL dynamics: looking for less inclusive variables

$$\langle p_T \rangle = \frac{1}{N}\sum_{i=1}^{N} |p_{Ti}|$$

$$\langle R_y \rangle = \frac{1}{N+1}\sum_{i=1}^{N+1} \frac{y_i}{y_{i-1}}$$

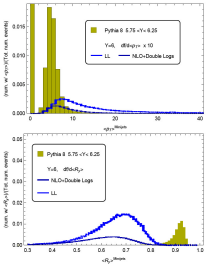

- Looking for multiple gluon emission along ladder characteristic of BFKL: number, p_T, rapidity distributions of "minijets"
- Comparison between BFKL-ex MC and pythia/herwig to find best variables: collaboration with A. Sabio Vera, D, Gordo, G. Chachamis, F. Deganutti, T. Raben

Figure: Slide by C.Royon

BFKL predictions in blue, BFKL predictions in green.

- $\langle R_y \rangle = \frac{1}{N+1}\sum_{i=1}^{N+1} \frac{y_i}{y_{i-1}}$ average of adjacent rapidity ratios.
- $\langle p_T \rangle = \frac{1}{N}\sum_{i=1}^{N} |p_{Ti}|$ " of mini-jet transverse momenta.

Path forward to be explored at future Snowmass Meetings?

Mueller Tang jets

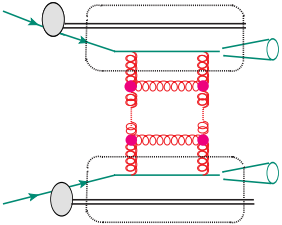

- No radiation into the rapidity gap suggests the color-singlet exchange contributes substantially to the jet-gap-jet cross section.
- The BFKL predictions for these processes have been studied at LL accuracy and *partially at NLL order*
- *Complete the NLL phenomenology analysis including the NLO impact factors. [Nucl. Phys. B887, 309 (2014), Nucl.Phys. B889, 549 (2014), PLB 735,168 (2014)].*

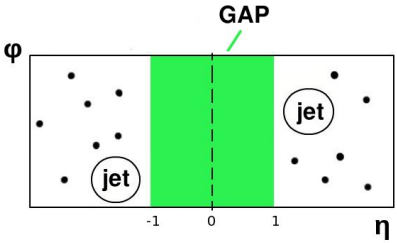

- Fixed rapidity gap $|\eta| < 1$, no charged particles *and* no photons or neutral hadrons with $p_T > 0.2$ GeV.
- Dijet events. At least 2 hard-jets $p_T^{jet} > 40$ GeV and $|\eta^{jet}| > 1.5$
- Jet radius $R_{jet} = 0.4$ and anti-k_t jet algorithm.

CMS and D0 analyses

7 *TeV* [EPJC 78,242 (2018)]

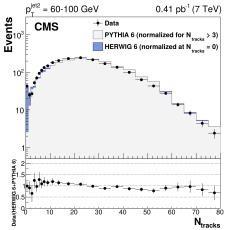

- Charged-particle multiplicity in the gap region between the tagged jets compared to PYTHIA and HERWIG predictions.
- HERWIG 6: include contributions from color singlet exchange (CSE), based on BFKL at LL.
- PYTHIA 6: inclusive dijets (tune Z2*), no-CSE.

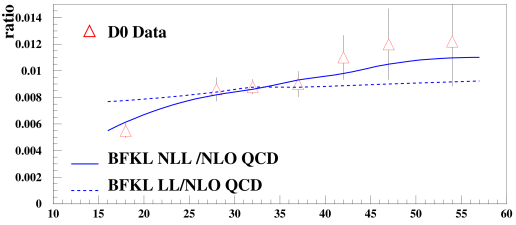

[O. Kepka, C. Marquet, C. Royon Phys.Rev. D83.034036 (2011)]

- Fraction of jet-gap-jet events vs inclusive dijets measured by D0 Coll. [Phys.Lett. B440 189 (1998)] well reproduced by BFKL estimates. **NLL order correction are necessary**
- Ratio $R = \frac{NLL^* BFKL}{NLOQCD}$ of jet-gap-jet events to inclusive dijet events as a function of p_t.
- NLL^* $\sim$ NLL (forward) Green Func. + collinear improvement. No NLO Imp. Factors
- Normalization fixed by gap survival probability $|S|^2 = 0.1$.

CMS analysis 13 TeV

See C.Baldenegro's talk given at Snowmass EF06 meeting on forward physics @ small-x QCD of June 17.

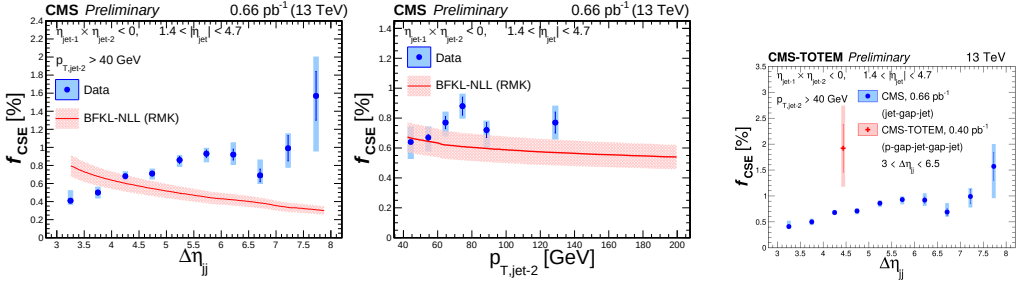

Unexpected rise in $\Delta\eta_{jj}$ and little dependence from p_{T_J}.

- Comparisons to Royon, Marquet, Kepka (RMK) model based on BFKL NLL calculations + LO impact factors [PRD83.034036], and survival probability $|S|^2 = 0.1$.
- RMK model predicts a decreasing fraction with increasing $\Delta\eta_{jj}$, in disagreement with the trend observed in data.
- Good to fair agreement to data for f_{CSE} vs p_{T_J}.

NLO impact factors

Several non trivial modifications to the theoretical description needed to accommodate the NLO corrections to the impact factors (IF).

Non-factorizable. NLO impact factors connect the Gluon Green functions over the "cut"

NLO impact factors have yet to be implemented for phenomenology studies to complete the NLO calculation (BFKL@NLL + impact factors@NLO).
Efforts by D. Colferai, F. Deganutti, C. Royon, T. Raben on this direction (private communication), and by U. of Munster coll. (M. Klasen, J. Salomon, P. Gonzlez, M. Kampshoff).

$$\frac{d\hat{\sigma}}{dJ_1 dJ_2 d^2\mathbf{q}} = |A(Y,q)|^2 \quad \Rightarrow \quad V_a(\mathbf{k}_1,\mathbf{k}_2,J_1,\mathbf{q}) \otimes G(\mathbf{k}_1,\mathbf{k'}_1,\mathbf{q},Y) \otimes G(\mathbf{k}_2,\mathbf{k'}_2,\mathbf{q},Y) \otimes V_b(\mathbf{k'}_1,\mathbf{k'}_2,J_2,\mathbf{q}),$$

$$A(Y,q) \sim V_a(q) V_b(q) \int d^2k d^2k' G(\mathbf{k},\mathbf{k'},\mathbf{q},Y) \qquad \tilde{G}\left(Y,\mathbf{q},\frac{k}{k'}\right) \propto \sum_n^{n\ even} \int d\nu \left[\frac{k^{*\bar{h}-2}}{k'^{\bar{h}-2}}\, {}_2F_1\left(1-h,2-h,2;\frac{k}{k'}\right)\ {}_2F_1\left(1-\bar{h},2-\bar{h},2;\frac{k'^*}{k^*}\right) + \{1 \leftrightarrow 2\}\right].$$

- From squared amplitude to multiple convolution between the the jet vertices and the GGFs.
- LO vertices are c-numbers and can be factorized out of the convolution.
- Average of GGF over the reggeon momenta is *remarkably* simple.

$$A(Y,q) \sim A(Y,q=0)\frac{4}{q^2}$$

GGF LL + NLO jet vertex

Breaking of high-energy factorization or uncontrolled observable definition?

$$\frac{d\hat{\sigma}}{dJ_1 dJ_2 d^2\mathbf{q}} = \int d^2k_1 d^2k_2 V^{NLO}(\mathbf{k}_1, \mathbf{k}_2, \mathbf{q}; J_1)\overline{G}(\mathbf{k}_1, \mathbf{q}, Y)\overline{G}(\mathbf{k}_2, \mathbf{q}, Y)V^{LO}(J_2, \mathbf{q})$$

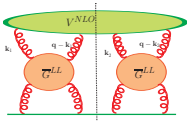

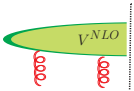

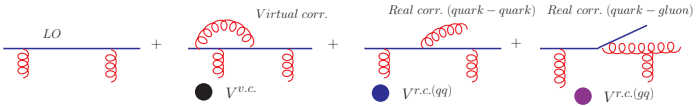

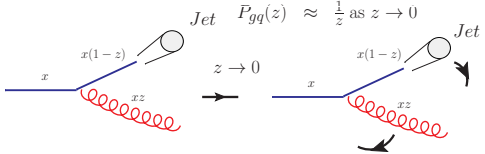

$$V^{r.c.(g,q)} = \int dz P_{gq}(z) \ldots \propto Y$$

All Y factors should be resummed in GGF

Preliminary Results

Comparing size of next-to-leading corrections.

- LO : $V^{LO} \otimes G^{LL} \otimes G^{LL} \otimes V^{LO}$
- NLO : $V^{NLO} \otimes G^{LL} \otimes G^{LL} \otimes V^{LO}$
- NLL : $V^{LO} \otimes G^{NLL} \otimes G^{NLL} \otimes V^{LO}$

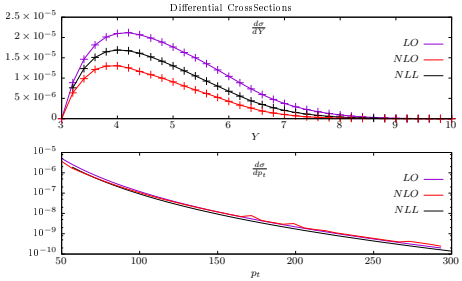

Beyond the back-to-back configuration. Marked peak in the vicinity of $\Delta\phi \sim \pi$ but not quite. The cross-section drops before the azimuthal diff. reaches π due to important subtractions.

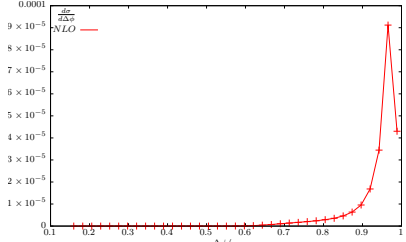

Conclusions

- QCD predictions even in the perturbative regimes are not fully understood (semi-hard regimes).
- BFKL NLL corrections are large and must be taken into account.
- The search for BFKL signature via Mueller-Navelet jet process is contaminated by important DGLAP contributions.
- Look for more exclusive observables that show a pronounced DGLAP suppression.
- BFKL predictions for Mueller-Tang observables remain inconclusive.
- Toward a phenomenological analysis at full NLL order.
- **Not only jets**: Drell-yang pairs, ρ and J/ψ ...

Backup

Previous fits and analysis

Fraction of jet-gap-jet events vs inclusive dijets measured by D0 Coll. [Phys.Lett. B440 189 (1998)] well reproduced by BFKL estimates. **NLL order correction are necessary**

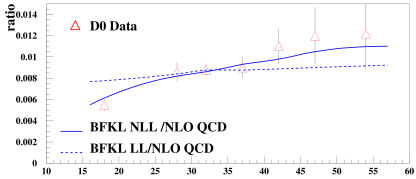

[O. Kepka, C. Marquet, C. Royon Phys.Rev. D83.034036 (2011)]

- Ratio $R = \frac{NLL^* BFKL}{NLOQCD}$ of jet-gap-jet events to inclusive dijet events as a function of p_t.
- NLL^* $\sim$ NLL (forward) Green Func. + collinear improvement. No NLO Imp. Factors
- Normalization fixed by gap survival probability $|S|^2 = 0.1$.

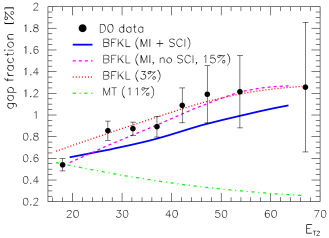

[R. Enberg, G. Ingelman, L. Motyka Phys.Lett.B524,273 (2002)]

- NLL^* BFKL predictions + soft rescattering corrections (EIM models) describe many features of the data (not so good for other observables).
- Different implementations of underlying event:
  Gap survival probability (S),
  Multiple interactions (MI),
  Soft colour interactions (SCI).

non-forward Gluon Green Function

The decision to keep just the pure NL contribution brings some simplification

$$\frac{d\hat{\sigma}}{dJ_1 dJ_2 d^2\mathbf{q}} = \int d^2k_1 d^2k_2 V^{NLO}(\mathbf{k}_1, \mathbf{k}_2, \mathbf{q}; J_1) \times \underbrace{\int d^2k'_1 G(\mathbf{k}_1, \mathbf{k}'_1, \mathbf{q}, Y)}_{\overline{G}(\mathbf{k}_1, \mathbf{q}, Y)} \underbrace{\int d^2k'_2 G(\mathbf{k}_2, \mathbf{k}'_2, \mathbf{q}, Y)}_{\overline{G}(\mathbf{k}_2, \mathbf{q}, Y)} V^{LO}(J_2, \mathbf{q})$$

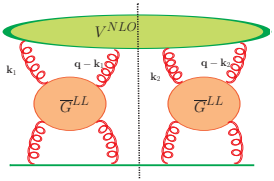

$$\bar{G}(x_1 x_2, q, \Delta\theta, \frac{k}{k'}) \propto \sum_m^{m\ even} \int d\nu \left[k^{*\bar{h}-2} k'^{h-2}\, {}_2F_1\left(1-h, 2-h, 2; -\frac{k}{k'}\right)\ {}_2F_1\left(1-\bar{h}, 2-\bar{h}, 2; -\frac{k'^*}{k^*}\right) + \{1 \leftrightarrow 2\} \right].$$

- Integrand is highly oscillatory and slowly falling with ν. $h = \frac{1+n}{2} + i\nu$
- Fast and reliable evaluation of ${}_2F_1(a, b, c; z)$ and for large $Im(a, b)$ notoriously difficult.
- To avoid numerical cancellations for large conformal spin even quadruple precision not enough.

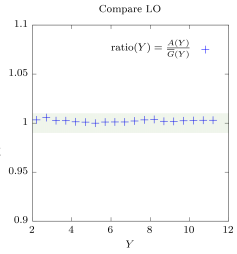

incorporating NLO impact factor

A full NLL/O calculation is within reach. NLO MT impact factors recently calculated [1406.5625,1409.6704]. Very complicated! (not in a factorizable form!)

But...only certain combinations of jet vertex and Green's function approximation orders contribute effectively to the NL order of the cross section. The most complicated combinations can be discarded because they are subleading.

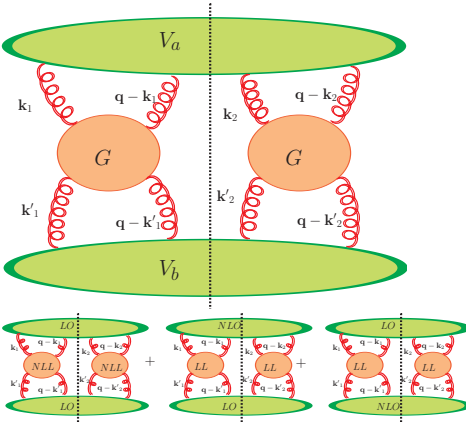

- GGF NLL + LO vertices. For this special case the general formula for the cross section can be expressed in a much simpler form because LL vertices are idependent from the reggeon momenta.
- GGF LL + LO vertex + NLO vertex. The non trivial dependence of the NLO jet vertex from the reggeon momenta introduces an important complication.
- GGF LL + both NLO vertices. Discarded because subleading.

NLO jet vertex

Peculiar characteristics of the NLO the jet vertex.

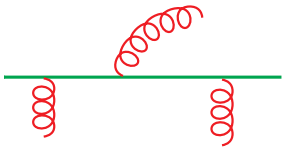

- The non trivial dependence from the reggeon momenta prevents the applicability of the mentioned simplification imposing the use of the general formula.
- Up to two partons can be emitted by the same vertex. Whether they are collinear enough to form the same jet or not depends on the choice of the jet reconstruction algorithm. (1) The two partons form the same jet or (2) one of the two has energy lower than the calorimeter threshold and so it is not detected.
- The soft parton emission in the prohibited region alter the alignment between the forward and the backward jet. The survival of the rapidity gap is assured imposing constraints to the additional parton emission. Jets not back to back anymore

$$\hat{\sigma}(q, Y) \to \hat{\sigma}(k_{J_1}, k_{J_2}, \theta_{J_2,J_2}, Y)$$

The additional soft emission is needed to assure the cancellation of the infrared divergences.

Numerical analysis

The decision to keep just the pure NL contribution brings some simplification

$$\frac{d\hat{\sigma}}{dJ_1 dJ_2 d^2\mathbf{q}} = \int d^2k_1 d^2k_2 V^1(\mathbf{k}_1, \mathbf{k}_2, \mathbf{q}; J_1) \times \underbrace{\int d^2k'_1 G(\mathbf{k}_1, \mathbf{k}'_1, \mathbf{q}, Y)}_{\overline{G}(\mathbf{k}_1, \mathbf{q}, Y)} \underbrace{\int d^2k'_2 G(\mathbf{k}_2, \mathbf{k}'_2, \mathbf{q}, Y)}_{\overline{G}(\mathbf{k}_2, \mathbf{q}, Y)} V^0(J_2, \mathbf{q})$$

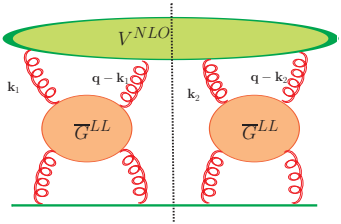

- Large increase in computation time due to the high-dimensional multiple integration.

The full form of the eigenfunction in momentum space is known [Bartels, Braun, Colferai, Vacca].

- The momentum dependence of the eigenfunction is expressed through hypergeometric functions in a region of parameter very sensible to numerical fluctuations. ${}_2F_1(a, b; c, z),\ a - b \in \mathbb{Z}^-$

Numerical analysis

- Calculation of the partonic cross section.
  (1) $\bar{G}$ as a grid of its parameters $\{k_i, q_j, \theta_l, Y_m\}$. It involves a numerical integration over ν and a sum over n for each set of the parameters.
  (2) Partonic cross section as the interpolation of $\bar{G}$ grids and the NLO vertex.

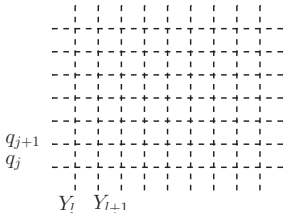

$$\frac{\hat{\sigma}(k_{J_1}, k_{J_2}, \theta_{J_1,J_2}, Y)}{dk_J dY} \propto \sum V(k_{1_i}, k_{2_j}, \theta_{1_n}, \theta_{2_m}, J)\bar{G}(k_{1_i}, q_r, \theta_{1_n}, Y_l)\bar{G}(k_{2_j}, q_r, \theta_{2_m}, Y_l)$$

- Dressing of the initial state and final state hadronization by Herwig
  (1) Proton-proton scattering $\frac{d\sigma^{pp\to JGJ}}{dx_1 dx_2 dq} \propto \sum_{a,b} f_a(x_1, k_{J_1}) f_b(x_2, k_{J_2})\hat{\sigma}(k_{J_1}, k_{J_2}, \theta_{J_1,J_2}, Y)$
  (2) Fitting of the cross section and its substitution by a sum of analytic functions of the fitting parameters.
  (3) Hadronization from the proto-jet to the detector with a matching procedure to remove the double counted diagrams. The error avoided by this subtraction is predicted to be of NL order.

BFKL

Balitsky, Fadin, Kuraev, Lipatov (BFKL) were the first to consider the Regge limit of QCD.
The large logs come from the integration over the longitudinal momentum fraction bounded by the outermost partons.
Sudakov parametrization $k_i = z_i p^+ + \bar{z}_i p^- + \mathbf{k}$, $p^+ = \frac{p_a}{\sqrt{2}}, p^- = \frac{p_b}{\sqrt{2}}$

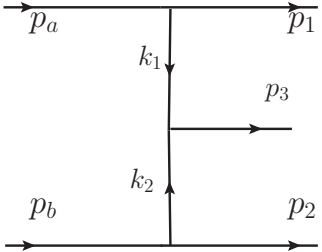

On shell conditions $\rightarrow (\mathbf{k}_1, \mathbf{k}_2, z_1)$, $\bar{z}_1 = \mathbf{k}_1/s$, $\bar{z}_2 = \mathbf{q}/z_1 s$.
Positive energies $E > 0 \rightarrow 1 > z_1 > z_2 > 0$.

$$\int d\Pi_3 \propto \int_{z_2}^{1} \frac{dz_1}{z_1} \int dz_2 \delta(z_2 - \mathbf{k}_2/s) = \log(\frac{s}{s_0})$$

Changing s_0 leaves the LL unaltered.

The amplitude is independent from the longitudinal fractions:

- Eikonal approximation $-ig\bar{u}(p_a - k_1)\gamma^\mu u(p_a) \simeq -2igp_a^\mu$.
- $k_1 \rightarrow z_1 p^+ + \mathbf{k}_2, k_1 \rightarrow \bar{z}_2 p^- + \mathbf{k}_2 \rightarrow k_1^2 = (z_1 p^+, 0, \mathbf{k}_1)^2 \rightarrow \frac{1}{k_1^2} \simeq -\frac{1}{\mathbf{k}_1^2}$.

For $s \gg t$ the predominant contribution comes from the strongly ordered region
$1 \gg z_1 \gg z_2 \gg 0 \rightarrow y_1 \gg y_3 \gg y_2$. $y_i = \log(\frac{z_i\sqrt{s}}{|\mathbf{k}_i|})$.

LL approximation: LO vertex

At LL accuracy the Gluon green function G resumms to all orders of perturbation theory the ladder diagrams composed by s-channel gluons connected to t-channel reggeizzed gluons through the Lipatov vertex. The normalization of the Gluon Green function fixes the jet vertex leading order.

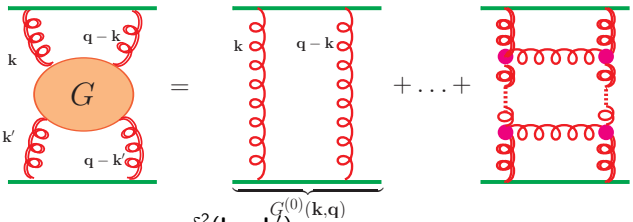

$$\lim_{Y\to 0} G(\mathbf{k},\mathbf{k}',\mathbf{q},Y) = G(\mathbf{k},\mathbf{k}',\mathbf{q},0) = \frac{\delta^2(\mathbf{k}-\mathbf{k}')}{\mathbf{k}^2(\mathbf{q}-\mathbf{k})^2}.$$

At this order, apart for the jet distribution function S that fixes the jet momentum, the jet vertex is a simple color factors (c-number)

$$V_a(x,\mathbf{q},x_J,\mathbf{k}_J) = S_J^0(x,\mathbf{q};x_J,\mathbf{k}_J)h_a^0,$$

$$h_a^0 = C_{q/g}^2\frac{\alpha_s^2}{N_c^2-1}, \qquad S_J^{(0)} = x\delta^2(\mathbf{k}_J-\mathbf{q})\delta(x_J-x).$$

The independence of the LO vertices from the reggeon momenta allow for considerable simplification.

details of NLO impact factor

Details of NLO impact factor

$$\frac{d\hat{V}^{(1)}(x,\boldsymbol{k},l_1,l_2;x_J,\boldsymbol{k}_J;M_{X,\max},s_0)}{dJ} =$$

$$= v_q^{(0)}\frac{\alpha_s}{2\pi}\left[S_J^{(2)}(\boldsymbol{k},x)\cdot\left[-\frac{\beta_0}{4}\left[\left\{\ln\left(\frac{l_1^2}{\mu^2}\right)+\ln\left(\frac{(l_1-k)^2}{\mu^2}\right)+\{1\leftrightarrow 2\}\right\}-\frac{20}{3}\right]-8C_f\right.\right.$$

$$+\frac{C_a}{2}\left[\left\{\frac{3}{2k^2}\left\{l_1^2\ln\left(\frac{(l_1-k)^2}{l_1^2}\right)+(l_1-k)^2\ln\left(\frac{l_1^2}{(l_1-k)^2}\right)-4|l_1||l_1-k|\phi_1\sin\phi_1\right\}\right.\right.$$

$$\left.\left.-\frac{3}{2}\left[\ln\left(\frac{l_1^2}{k^2}\right)+\ln\left(\frac{(l_1-k)^2}{k^2}\right)\right]-\ln\left(\frac{l_1^2}{k^2}\right)\ln\left(\frac{(l_1-k)^2}{s_0}\right)-\ln\left(\frac{(l_1-k)^2}{k^2}\right)\ln\left(\frac{l_1^2}{s_0}\right)-2\phi_1^2+\{1\leftrightarrow 2\}\right\}+2\pi^2+\frac{14}{3}\right]\right]$$

$$+\int_{z_0}^1 dz\left\{\ln\frac{\lambda^2}{\mu_F^2}S_J^{(2)}(\boldsymbol{k},zx)\left[P_{qq}(z)+\frac{C_a^2}{C_f^2}P_{gq}(z)\right]+\left[(1-z)\left[1-\frac{2}{z}\frac{C_a^2}{C_f^2}\right]+2(1+z^2)\left(\frac{\ln(1-z)}{1-z}\right)_+\right]S_J^{(2)}(\boldsymbol{k},zx)+4S_J^{(2)}(\boldsymbol{k},x)\right\}$$

$$+\int_0^1 dz\int\frac{d^2\boldsymbol{q}}{\pi}\left[P_{qq}(z)\Theta\left(\hat{M}^2_{X,\max}-\frac{(\boldsymbol{p}-z\boldsymbol{k})^2}{z(1-z)}\right)\Theta\left(\frac{|\boldsymbol{q}|}{1-z}-\lambda\right)\right.$$

$$\times\frac{\boldsymbol{k}^2}{\boldsymbol{q}^2(\boldsymbol{p}-z\boldsymbol{k})^2}S_J^{(3)}(\boldsymbol{p},\boldsymbol{q},(1-z)x,x)+\Theta\left(\hat{M}^2_{X,\max}-\frac{\boldsymbol{\Delta}^2}{z(1-z)}\right)S_J^{(3)}(\boldsymbol{p},\boldsymbol{q},zx,x)P_{gq}(z)$$

$$\left.\left.\times\left\{\frac{C_a}{C_f}[J_1(\boldsymbol{q},\boldsymbol{k},l_1,z)+J_1(\boldsymbol{q},\boldsymbol{k},l_2,z)]+\frac{C_a^2}{C_f^2}J_2(\boldsymbol{q},\boldsymbol{k},l_1,l_2)\Theta(\boldsymbol{p}^2-\lambda^2)\right\}\right]\right]$$

NLO impact factors

In general the cross section for these processes is given as a multiple convolution between the the jet vertices and the GGFs.

$$\frac{d\hat{\sigma}}{d\mathcal{J}_1 d\mathcal{J}_2 d^2\mathbf{q}} = \int d^2\mathbf{k}_1 d^2\mathbf{k'}_1 d^2\mathbf{k}_2 d^2\mathbf{k'}_2 V_a(\mathbf{k}_1, \mathbf{k}_2, \mathcal{J}_1, \mathbf{q}) \times$$
$$G(\mathbf{k}_1, \mathbf{k'}_1, \mathbf{q}, Y) G(\mathbf{k}_2, \mathbf{k'}_2, \mathbf{q}, Y) V_b(\mathbf{k'}_1, \mathbf{k'}_2, \mathcal{J}_2, \mathbf{q}), \qquad \mathcal{J} = \{\mathbf{k}_{\mathcal{J}}, x_{\mathcal{J}}\}.$$

Jet Functions for NLO impact factor

$$J_1(q, k, l, z) = \frac{1}{2}\frac{k^2}{(q-k)^2}\left(\frac{(1-z)^2}{(q-zk)^2} - \frac{1}{q^2}\right) - \frac{1}{4}\frac{1}{(q-l)^2}\left(\frac{(l-z\cdot k)^2}{(q-zk)^2} - \frac{l^2}{q^2}\right)$$
$$- \frac{1}{4}\frac{1}{(q-k+l)^2}\left(\frac{(l-(1-z)k)^2}{(q-zk)^2} - \frac{(l-k)^2}{q^2}\right);$$

$$J_2(q, k, l_1, l_2) = \frac{1}{4}\Big[\frac{l_1^2}{(q-k)^2(q-k+l_1)^2} + \frac{(k-l_1)^2}{(q-k)^2(q-l_1)^2}$$
$$+ \frac{l_2^2}{(q-k)^2(q-k+l_2)^2} + \frac{(k-l_2)^2}{(q-k)^2(q-l_2)^2} - \frac{1}{2}\Big(\frac{(l_1-l_2)^2}{(q-l_1)^2(q-l_2)^2}$$
$$+ \frac{(k-l_1-l_2)^2}{(q-k+l_1)^2(q-l_2)^2} + \frac{(k-l_1-l_2)^2}{(q-k+l_2)^2(q-l_1)^2} + \frac{(l_1-l_2)^2}{(q-k+l_1)^2(q-k+l_2)^2}\Big)\Big].$$

LL approximation: Non forward gluon Green function

The GGF is given by the Mellin transform of the function f_ω which is the solution of the BFKL equation. The solution of the non forward BFKL equation is more naturally expressed in the impact parameter space.

$$G(\mathbf{k},\mathbf{k}',\mathbf{q},Y)=\int_{-i\,\mathrm{inf}}^{+i\,\mathrm{inf}}\frac{d\omega}{2\pi i}e^{Y\omega}f_\omega(\mathbf{k},\mathbf{k}',\mathbf{q})$$

$$f_\omega(\rho_1,\rho_2,\rho_1',\rho_2')=\frac{1}{(2\pi)^6}\sum_{n=-\,\mathrm{inf}}^{+\,\mathrm{inf}}\int_{-\,\mathrm{inf}}^{+inf}d\nu\frac{R_{n\nu}}{\omega-\omega(n,\nu)}E^*_{n\nu}(\rho_1',\rho_2')E_{n\nu}(\rho_1,\rho_2)$$

$$E_{n\nu}(\rho_1,\rho_2)=\underbrace{\left(\frac{\rho_1-\rho_2}{\rho_1\rho_2}\right)^h\left(\frac{\rho_1^*-\rho_2^*}{\rho_1^*\rho_2^*}\right)^{\bar h}}_{\text{Lipatov term}}\quad\underbrace{-\left(\frac{1}{\rho_2}\right)^h\left(\frac{1}{\rho_2^*}\right)^{\bar h}-\left(\frac{-1}{\rho_1}\right)^h\left(\frac{-1}{\rho_1^*}\right)^{\bar h}}_{\text{Mueller-Tang correction}}$$

$E_{n\nu}$ are the eigenfunctions in the impact parameter space.
The GGF in momentum space is recovered applying a Fourier transformation to the eigenfunctions.

$$\tilde E_{n\nu}(\mathbf{k},\mathbf{q})=\int\frac{d^2r_1d^2r_2}{(2\pi)^4}E_{n\nu}(\rho_1,\rho_2)e^{i(\mathbf{k}\cdot\mathbf{r}_1+(\mathbf{q}-\mathbf{k})\cdot\mathbf{r}_2)}$$

Mueller Navelet jets at NLL

At NLL the approximation is refined including the terms $\propto \alpha_s^n \log^{(n-1)}(\frac{s}{-t})$.

- Larger variety of Feynman diagrams give rise to a much more complex iterating structure
- LL order diagrams evaluated in a broader kinematic domain
  Up to two partons are close in rapidity (Quasi-MRK).

$$y_1' \gg y_1 \gg \cdots \gg y_i \simeq y_{i+1} \gg \cdots \gg y_n \gg y_2'$$

The jet vertex gets its part of the radiative corrections

$$V(\mathbf{k}_J, x_j, \mathbf{k}) = V^{(0)}(\mathbf{k}_J, x_j, \mathbf{k}) + \alpha_s V^{(1)}(\mathbf{k}_J, x_j, \mathbf{k})$$

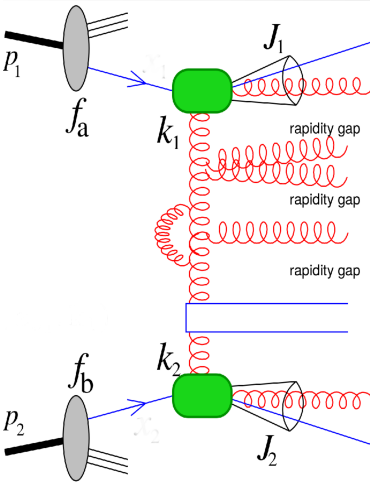

- NL corrections to the jet vertex calculated by Bartels, Colferai and Vacca (BCV).
- QMRK $\rightarrow$ up to **two** outgoing parton per vertex

BFKL resummation

Balitsky, Fadin, Kuraev, Lipatov (BFKL) considered the Regge limit of QCD.

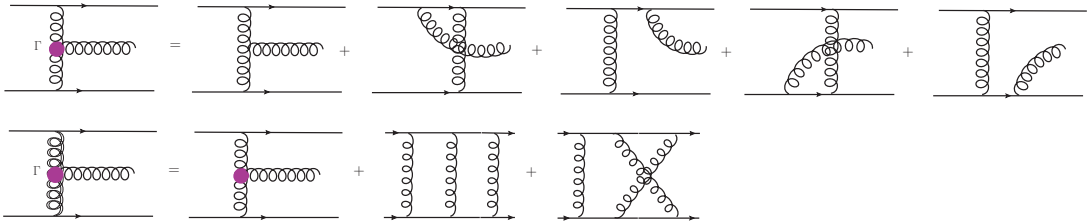

Diagrams enhanced by $\log^1 s/t$ grouped according to the number of lines cut by Cutkosky.

- *real* corrections collected into the **Lipatox vertex** $\Gamma^{\mu\nu}_{\rho}$.
- *virtual* corrections contribute to the **gluon reggeization**.
  t-channel gluon propagators acquire a power dependence:

$$\frac{1}{t} \to \frac{1}{t}\left(1 + \epsilon(t)\log\left(\frac{s}{t}\right) + \frac{\epsilon^2(t)}{2}\log^2\left(\frac{s}{t}\right) + \dots\right) = \frac{1}{t}\left(\frac{s}{t}\right)^{\epsilon(t)}$$

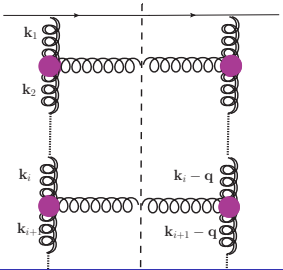

At LL simple repeating structure:

- Ladder diagrams: t-channel Reggeized gluons connected to s-channel gluons